COBEM 2021 26th International Congress of Mechanical Engineering
ABCM Associação Brasileira de Engenharia e Ciências Mecânicas
November 22-26, 2021, Virtual Congress, Brazil

COB-2021-1829
PARAMETER-DEPENDENT SURFACE-TO-AIR MISSILE AUTOPILOT DESIGN

Yuri Marchetti Tavares
Marinha do Brasil.
yurimtavares@yahoo.com.br

Jacques Waldmann
Instituto Tecnológico de Aeronáutica, Departamento de Engenharia Eletrônica e Computação, Sistemas e Controle.
jacques.waldmann.yaari@gmail.com

Abstract. *High performance missiles impose a challenge to autopilot design with guaranteed high performance and robustness over a large range of operational conditions that affect flight dynamics. Classic gain-scheduling designs have been successful in practice but do not provide theoretically guaranteed characteristics. We propose here a gain-scheduled parameter-dependent autopilot based on four-block loop-shaping H_∞ control. The missile design model is described as a polytopic linear parameter varying (LPV) system that depends on time-varying parameters, which we assume are measured in real-time. The dynamic output feedback controller is based on H_∞ optimization. For loop-shaping, we propose weights with matched parameter dependency as the LPV plant model to equalize the singular-values' frequency response and attain feasible LMI solution at each polytope vertex. The proposed method is tested with nonlinear 6-degree-of-freedom simulations of a surface-to-air missile (SAM) against an airborne target that resulted in an average miss distance less than 4 m for the simulated scenarios with successful impact rating above 97%.*

Keywords: *Autopilot, LPV, H_∞ control, missile, loop-shaping*

1. INTRODUCTION

Increasing high performance requirements and greater maneuverability of recent airborne targets demand higher performance from modern missiles. The autopilot has an important role in the missile control system as it relates to maintaining stability and performance over a wide range of plant parameters such as speed, angle-of-attack, and especially uncertainty in aerodynamic coefficients (Prempain *et al.*, 2001). Whereas classic gain-scheduling designs have been successful in practice, robustness and performance characteristics are not guaranteed theoretically (Shamma and Athans, 1991). More recently, linear parameter varying (LPV) systems control techniques have attracted attention because of their robust characteristics (Song *et al.*, 2013).

LPV systems can be understood as time-varying linear systems that result from linearizing the plant dynamics along the trajectory of relevant parameters that traverse a polytopic domain (Apkarian *et al.*, 1995b). Assuming that such parameters are measured in real time, the design of gain-scheduled controllers explores matching the parameter dependence that dictates the plant dynamics and thus such controllers can improve system performance and robustness.

The simultaneous optimization of robust stability and robust performance while minimizing the control action is not a simple task. H_∞ control of a multivariable LPV system is one approach to achieve this objective. Furthermore, H_∞ loop-shaping allows for the application of concepts underlying traditional loop-shaping to multivariable systems. Then a linear matrix inequalities (LMI) approach assumes that convex optimization conditions hold to yield the controller synthesis.

We propose a gain-scheduled parameter-dependent autopilot based on four-block loop-shaping H_∞ control with the above LPV approach. The controller is dynamic and the design is based in the linearized missile dynamic model along the parameter trajectory. Tests were performed by means of the nonlinear simulation of a 6-degree-of-freedom surface-to-air missile (SAM). As just a few output measurements are available in flight and the short-duration intercept game calls for a rather fast closed-loop guidance and autopilot dynamics, we focus on exploring the benefits and limitations of output feedback in opposition to the feedback of the full estimated state.

This paper is structured as follows. Some of the theoretical concepts of loop-shaping H_∞ control and LPV systems are reviewed in Section 2. The proposed method for the parameter-dependent controller design is presented in Section 3. The missile nonlinear model and the linearized model along the parameter trajectory are detailed in Section 4. The design of the autopilot and the simulation results are registered in Section 5. Finally, conclusions are given in Section 6.

The notation used in this paper is standard: matrices and vectors are written in boldface (uppercase and lowercase, respectively), $\boldsymbol{A} > 0$ means that matrix $\boldsymbol{A}$ is positive definite, $\mathbb{R}^{m\times n}$ denotes the set of $m \times n$ real matrices, $\mathbb{R}^n$ denotes the set of real vectors with dimension n. $\boldsymbol{I}$ is the identity matrix with appropriate dimensions and $\boldsymbol{I}_n$ is the identity matrix $\in \mathbb{R}^{n\times n}$. $\boldsymbol{G} = \left[\begin{array}{c|c} \boldsymbol{A} & \boldsymbol{B} \\ \hline \boldsymbol{C} & \boldsymbol{D} \end{array}\right]$ represents a state-space realization of a system whose transfer function is *G(s)* $=$ $\boldsymbol{C}(s\boldsymbol{I}-\boldsymbol{A})^{-1}\boldsymbol{B}+\boldsymbol{D}$. $G^*(s)$ is a shorthand for $G^T(-s)$. The symbol $\triangleq$ means "equal by definition".

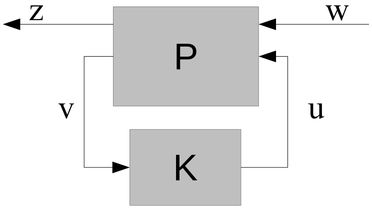

Figure 1. General control problem diagram.

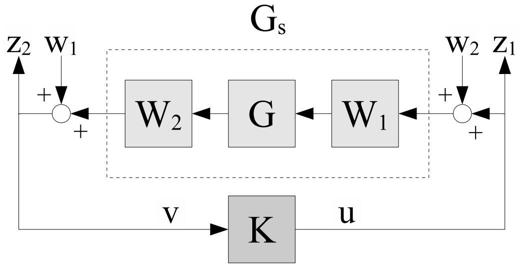

Figure 2. Diagram of four-block loop-shaping framework.

2. PRELIMINARIES

2.1 Output feedback dynamic H$_\infty$ control

Let a dynamic system be described as generalized plant $\boldsymbol{P}$, as illustrated in the general control problem in Figure 1. A state-space realization is:

$$\boldsymbol{P} \triangleq \left[\begin{array}{c|cc} \boldsymbol{A} & \boldsymbol{B}_1 & \boldsymbol{B}_2 \\ \hline \boldsymbol{C}_1 & \boldsymbol{D}_{11} & \boldsymbol{D}_{12} \\ \boldsymbol{C}_2 & \boldsymbol{D}_{21} & \boldsymbol{D}_{22} \end{array}\right] \rightarrow \begin{bmatrix} \dot{\boldsymbol{x}} \\ \boldsymbol{z} \\ \boldsymbol{v} \end{bmatrix} = \left[\begin{array}{c|cc} \boldsymbol{A} & \boldsymbol{B}_1 & \boldsymbol{B}_2 \\ \hline \boldsymbol{C}_1 & \boldsymbol{D}_{11} & \boldsymbol{D}_{12} \\ \boldsymbol{C}_2 & \boldsymbol{D}_{21} & \boldsymbol{D}_{22} \end{array}\right] \begin{bmatrix} \boldsymbol{x} \\ \boldsymbol{w} \\ \boldsymbol{u} \end{bmatrix} \tag{1}$$

where $\boldsymbol{x} \in \mathbb{R}^n$ are the states, $\boldsymbol{w} \in \mathbb{R}^{n_w}$ are the exogenous inputs (like disturbances and commands), $\boldsymbol{u} \in \mathbb{R}^{n_u}$ are the control inputs , $\boldsymbol{z} \in \mathbb{R}^{n_z}$ are the controlled outputs (usually are the error signals), $\boldsymbol{v} \in \mathbb{R}^{n_v}$ are the measured outputs. The closed-loop transfer function from $\boldsymbol{w}$ to $\boldsymbol{z}$ is given by Linear Fractional Transformation (LFT) $\boldsymbol{z} = F_l(\boldsymbol{P},\boldsymbol{K})\boldsymbol{w}$ for a controller $\boldsymbol{K}$ defined in state-space as:

$$\boldsymbol{K} \triangleq \left[\begin{array}{c|c} \boldsymbol{A}_k & \boldsymbol{B}_k \\ \hline \boldsymbol{C}_k & \boldsymbol{D}_k \end{array}\right] \rightarrow \begin{bmatrix} \dot{\boldsymbol{x}}_k \\ \boldsymbol{u} \end{bmatrix} = \left[\begin{array}{c|c} \boldsymbol{A}_k & \boldsymbol{B}_k \\ \hline \boldsymbol{C}_k & \boldsymbol{D}_k \end{array}\right] \begin{bmatrix} \boldsymbol{x}_k \\ \boldsymbol{v} \end{bmatrix} \tag{2}$$

where $\boldsymbol{x}_k \in \mathbb{R}^k$ are the controller states and the control is $\boldsymbol{u} = K(s)\boldsymbol{v}$. Considering $\boldsymbol{D}_{22} = 0$, the closed-loop transfer function from $\boldsymbol{w}$ to $\boldsymbol{z}$ is defined in state-space as:

$$\boldsymbol{T}_{zw} = \left[\begin{array}{c|c} \boldsymbol{A}_{cl} & \boldsymbol{B}_{cl} \\ \hline \boldsymbol{C}_{cl} & \boldsymbol{D}_{cl} \end{array}\right] = \left[\begin{array}{cc|c} \boldsymbol{A}+\boldsymbol{B}_2\boldsymbol{D}_k\boldsymbol{C}_2 & \boldsymbol{B}_2\boldsymbol{C}_k & \boldsymbol{B}_1+\boldsymbol{B}_2\boldsymbol{D}_k\boldsymbol{D}_{21} \\ \boldsymbol{B}_k\boldsymbol{C}_2 & \boldsymbol{A}_k & \boldsymbol{B}_k\boldsymbol{D}_{21} \\ \hline \boldsymbol{C}_1+\boldsymbol{D}_{12}\boldsymbol{D}_k\boldsymbol{C}_2 & \boldsymbol{D}_{12}\boldsymbol{C}_k & \boldsymbol{D}_{11}+\boldsymbol{D}_{12}\boldsymbol{D}_k\boldsymbol{D}_{21} \end{array}\right] \rightarrow \left[\begin{array}{c} \dot{\boldsymbol{x}} \\ \dot{\boldsymbol{x}}_k \\ \hline \boldsymbol{z} \end{array}\right] = \boldsymbol{T}_{zw} \left[\begin{array}{c} \boldsymbol{x} \\ \boldsymbol{x}_k \\ \hline \boldsymbol{w} \end{array}\right] \tag{3}$$

The H_∞ control problem involves the H_∞-norm minimization of the closed-loop system $\boldsymbol{T}_{zw}$ (Skogestad and Postlethwaite, 2001). Usually, suboptimal controllers are cheaper to obtain and have nice properties (like lower bandwidth) than the optimal ones (Zhou *et al.*, 1996). For linear time-invariant (LTI) systems, Scherer *et al.* (1997) presents a solution for an output feedback dynamic H_∞ suboptimal controller *K(s)* using LMI and the well known Bounded Real Lemma.

2.2 Four-block loop-shaping H$_\infty$ control

Loop-shaping H_∞ control theory combines the classic loop-shaping performance/robustness trade-off with an effective H_∞ design to robustly stabilize the feedback system. The method by McFarlane and Glover (1990) using Riccati equations has two main stages: 1) using a pre-compensator $W_1(s)$ and a post-compensator $W_2(s)$, the open-loop frequency response is shaped to yield the desired singular values. The nominal plant and the compensators are combined to form the shaped plant $G_s(s) = W_2(s)G(s)W_1(s)$. $W_1(s)$ and $W_2(s)$ are chosen such that $G_s(s)$ contains no hidden modes. 2) $G_s(s)$ is robustly stabilized by $K(s)$, obtained via H_∞-optimization and considering uncertainties in the normalized coprime factorization. The final feedback controller for nominal plant $G(s)$ combines the stabilizing controller $K(s)$ with the shaping functions such that $K_F(s) = W_1(s)K(s)W_2(s)$. The advantages of the loop-shaping H_∞ control are (Hiret *et al.*, 1999): (a) preservation of physical meaning because of open-loop shaping; (b) stability and robustness guarantee; and (c) performance of the closed-loop system.

Consider the normalized left coprime factorization of $G_s(s) = \tilde{M}(s)^{-1}\tilde{N}(s)$. Since the pair $\tilde{M}(s)$ and $\tilde{N}(s)$ is a normalized left coprime factorization of $G_s(s)$, we have $\begin{bmatrix}\tilde{M}(s) & \tilde{N}(s)\end{bmatrix}\begin{bmatrix}\tilde{M}(s) & \tilde{N}(s)\end{bmatrix}^* = I$ and $\left\|\begin{bmatrix}\tilde{M}(s) & \tilde{N}(s)\end{bmatrix}\right\|_\infty = 1$ and a controller solves the normalized left coprime factor robust stabilization problem if and only if it solves the following H_∞ control problem (Zhou *et al.*, 1996, lemma 18.4 and corollary 18.5):

$$\|T_{zw}(s)\|_\infty = \left\|\begin{bmatrix}K(s)\\ I\end{bmatrix}(I + G_s(s)K(s))^{-1}\begin{bmatrix}I & G_s(s)\end{bmatrix}\right\|_\infty < \frac{1}{\epsilon_{max}} = \gamma \tag{4}$$

where ϵ_{max} is the maximum achievable robust stability margin (McFarlane and Glover, 1990). This robust stabilization objective can also be interpreted as a problem of minimizing the H_∞-norm of the frequency weighted gain from two exogenous signal vectors ($\boldsymbol{w}_1$ and $\boldsymbol{w}_2$) to two objective signal vectors ($\boldsymbol{z}_1$ and $\boldsymbol{z}_2$), and is called the four-block problem (see, e.g., McFarlane and Glover (1992)), shown in Figure 2. Define the shaped plant in state-space as $\boldsymbol{G}_s \triangleq \left[\begin{array}{c|c}\boldsymbol{A}_{GS} & \boldsymbol{B}_{GS}\\ \hline \boldsymbol{C}_{GS} & 0\end{array}\right]$. Then, its generalized plant $\boldsymbol{P}_{GS}$ of the four-block loop-shaping framework is given by (Natesan *et al.*, 2007):

$$\boldsymbol{P}_{GS} = \left[\begin{array}{c|cc}\boldsymbol{A} & \boldsymbol{B}_1 & \boldsymbol{B}_2\\ \hline \boldsymbol{C}_1 & \boldsymbol{D}_{11} & \boldsymbol{D}_{12}\\ \boldsymbol{C}_2 & \boldsymbol{D}_{21} & \boldsymbol{D}_{22}\end{array}\right] = \left[\begin{array}{c|cc}\boldsymbol{A}_{GS} & \begin{bmatrix}0 & \boldsymbol{B}_{GS}\end{bmatrix} & \boldsymbol{B}_{GS}\\ \hline \begin{bmatrix}0\\ \boldsymbol{C}_{GS}\end{bmatrix} & \begin{bmatrix}0 & 0\\ \boldsymbol{I} & 0\end{bmatrix} & \begin{bmatrix}\boldsymbol{I}\\ 0\end{bmatrix}\\ \boldsymbol{C}_{GS} & \begin{bmatrix}\boldsymbol{I} & 0\end{bmatrix} & 0\end{array}\right] \rightarrow \begin{bmatrix}\dot{\boldsymbol{x}}\\ \boldsymbol{z}_1\\ \boldsymbol{z}_2\\ \boldsymbol{v}\end{bmatrix} = \left[\begin{array}{c|cc}\boldsymbol{A}_{GS} & \begin{bmatrix}0 & \boldsymbol{B}_{GS}\end{bmatrix} & \boldsymbol{B}_{GS}\\ \hline \begin{bmatrix}0\\ \boldsymbol{C}_{GS}\end{bmatrix} & \begin{bmatrix}0 & 0\\ \boldsymbol{I} & 0\end{bmatrix} & \begin{bmatrix}\boldsymbol{I}\\ 0\end{bmatrix}\\ \boldsymbol{C}_{GS} & \begin{bmatrix}\boldsymbol{I} & 0\end{bmatrix} & 0\end{array}\right]\begin{bmatrix}\boldsymbol{x}\\ \boldsymbol{w}_1\\ \boldsymbol{w}_2\\ \boldsymbol{u}\end{bmatrix} \tag{5}$$

2.3 Linear parameter varying systems

Linear parameter varying systems are special instances of linear time-varying (LTV) systems when the state-space matrices depend on time-varying parameters vector $\theta(t)$. A state-space realization has the form:

$$\begin{aligned}\dot{\boldsymbol{x}} &= \boldsymbol{A}(\theta(t))\boldsymbol{x} + \boldsymbol{B}(\theta(t))\boldsymbol{u}\\ \boldsymbol{y} &= \boldsymbol{C}(\theta(t))\boldsymbol{x} + \boldsymbol{D}(\theta(t))\boldsymbol{u}\end{aligned} \tag{6}$$

where $\boldsymbol{x} \in \mathbb{R}^n$ are the states, $\boldsymbol{u} \in \mathbb{R}^{n_u}$ is the control vector, $\boldsymbol{y} \in \mathbb{R}^{n_y}$ are the outputs and $\theta(t) \in \mathbb{R}^p$ is the vector of time-varying parameters. Apkarian and Gahinet (1995a) present two interesting ways to interpret LPV systems: 1) they can be seen as LTI plants subject to time-varying parametric uncertainty $\theta(t)$; or 2) they can be the result of nonlinear plants linearization along the trajectories of the parameter $\theta(t)$. In this second class, parameter $\theta(t)$ is no longer considered uncertain and needs to be measured. The LPV control strategy can design time-varying $K(\theta(t))$ controllers with matched plant dependence on $\theta(t)$ to improve performance:

$$\begin{aligned}\dot{\boldsymbol{x}}_k &= \boldsymbol{A}_k(\theta(t))\boldsymbol{x}_k + \boldsymbol{B}_k(\theta(t))\boldsymbol{v}\\ \boldsymbol{u} &= \boldsymbol{C}_k(\theta(t))\boldsymbol{x}_k + \boldsymbol{D}_k(\theta(t))\boldsymbol{v}\end{aligned} \tag{7}$$

where $\boldsymbol{x}_k \in \mathbb{R}^k$ are the controller states, $\boldsymbol{v} \in \mathbb{R}^{n_v}$ represents the measurement vector and $\boldsymbol{u} \in \mathbb{R}^{n_u}$ is the control vector. Clearly, this approach is restricted to LPV plants where $\theta(t)$ is measured in real time.

The LPV systems discussed here are those in which $\boldsymbol{A}(\theta(t))$, $\boldsymbol{B}(\theta(t))$, $\boldsymbol{C}(\theta(t))$ and $\boldsymbol{D}(\theta(t))$ have an affine dependency on $\theta(t)$ that varies on a convex polytope of vertices $\xi_1, \xi_2, \dots, \xi_r \in \mathbb{R}^p$:

$$\theta(t) \in \Theta \triangleq Co\{\xi_1, \xi_2, ..., \xi_r\} \triangleq \{\textstyle\sum_{i=1}^r a_i\xi_i,\ a_i \geq 0,\ \sum_{i=1}^r a_i = 1\}, \quad r = 2^p \tag{8}$$

Therefore, the LPV system matrices can be described as follows:

$$\begin{aligned}&\begin{bmatrix}\boldsymbol{A}(\theta) & \boldsymbol{B}(\theta)\\ \boldsymbol{C}(\theta) & \boldsymbol{D}(\theta)\end{bmatrix} \in Co\left\{\begin{bmatrix}\boldsymbol{A}_i & \boldsymbol{B}_i\\ \boldsymbol{C}_i & \boldsymbol{D}_i\end{bmatrix} \triangleq \begin{bmatrix}\boldsymbol{A}(\xi_i) & \boldsymbol{B}(\xi_i)\\ \boldsymbol{C}(\xi_i) & \boldsymbol{D}(\xi_i)\end{bmatrix}\right\},\ i = 1, \dots, r\\ &\begin{bmatrix}\boldsymbol{A}(\theta) & \boldsymbol{B}(\theta)\\ \boldsymbol{C}(\theta) & \boldsymbol{D}(\theta)\end{bmatrix} \triangleq \textstyle\sum_{i=1}^r a_i\begin{bmatrix}\boldsymbol{A}_i & \boldsymbol{B}_i\\ \boldsymbol{C}_i & \boldsymbol{D}_i\end{bmatrix},\ a_i \geq 0,\ \sum_{i=1}^r a_i = 1\end{aligned} \tag{9}$$

and the controller matrices are given by:

$$\begin{aligned}&\begin{bmatrix}\boldsymbol{A}_k(\theta) & \boldsymbol{B}_k(\theta)\\ \boldsymbol{C}_k(\theta) & \boldsymbol{D}_k(\theta)\end{bmatrix} \in Co\left\{\begin{bmatrix}\boldsymbol{A}_{ki} & \boldsymbol{B}_{ki}\\ \boldsymbol{C}_{ki} & \boldsymbol{D}_{ki}\end{bmatrix} \triangleq \begin{bmatrix}\boldsymbol{A}_k(\xi_i) & \boldsymbol{B}_k(\xi_i)\\ \boldsymbol{C}_k(\xi_i) & \boldsymbol{D}_k(\xi_i)\end{bmatrix}\right\},\ i = 1, \dots, r\\ &\begin{bmatrix}\boldsymbol{A}_k(\theta) & \boldsymbol{B}_k(\theta)\\ \boldsymbol{C}_k(\theta) & \boldsymbol{D}_k(\theta)\end{bmatrix} \triangleq \textstyle\sum_{i=1}^r a_i\begin{bmatrix}\boldsymbol{A}_{ki} & \boldsymbol{B}_{ki}\\ \boldsymbol{C}_{ki} & \boldsymbol{D}_{ki}\end{bmatrix},\ a_i \geq 0,\ \sum_{i=1}^r a_i = 1\end{aligned} \tag{10}$$

Apkarian and Gahinet (1995a) refer to LPV plants described in the Eqs. (8) and (9) as polytopic LPV systems. An LPV system reduces to an LTI system when the parameter $\theta(t)$ is frozen to a constant value (Biannic and Apkarian, 1999).

2.4 LPV approach applied to output feedback dynamic H_∞ control

The synthesis condition of the output feedback dynamic H_∞ controller proposed by Scherer *et al.* (1997) for LTI systems can be directly extended to the LPV case where the generalized plant has the form of polytopic system

$$\boldsymbol{P}(\theta) \triangleq \left[\begin{array}{c|cc} \boldsymbol{A}(\theta) & \boldsymbol{B}_1 & \boldsymbol{B}_2 \\ \hline \boldsymbol{C}_1 & \boldsymbol{D}_{11} & \boldsymbol{D}_{12} \\ \boldsymbol{C}_2 & \boldsymbol{D}_{21} & \boldsymbol{D}_{22}=0 \end{array}\right] = \sum_{i=1}^{r} a_i \left[\begin{array}{c|cc} \boldsymbol{A}_i & \boldsymbol{B}_1 & \boldsymbol{B}_2 \\ \hline \boldsymbol{C}_1 & \boldsymbol{D}_{11} & \boldsymbol{D}_{12} \\ \boldsymbol{C}_2 & \boldsymbol{D}_{21} & 0 \end{array}\right] \tag{11}$$

In this situation, the controller and following variables may be defined in a polytopic description: $\boldsymbol{F}(\theta) = \sum_{i=1}^{r} a_i \boldsymbol{F}_i$; $\boldsymbol{L}(\theta) = \sum_{i=1}^{r} a_i \boldsymbol{L}_i$; $\boldsymbol{Q}(\theta) = \sum_{i=1}^{r} a_i \boldsymbol{Q}_i$; $\boldsymbol{\Psi}(\theta) = \sum_{i=1}^{r} a_i \boldsymbol{\Psi}_i$. Thus, there is an output feedback dynamic parameter-dependent controller $\boldsymbol{K}(\theta)$, such that $\|\boldsymbol{T}_{zw}\|_\infty < \gamma$ for all trajectories of $\theta(t)$ in the polytope Θ, if and only if there are symmetric matrices $\boldsymbol{R} \in \mathbb{R}^{n\times n}$ and $\boldsymbol{S} \in \mathbb{R}^{n\times n}$ that satisfy following LMI:

$$\begin{bmatrix} \boldsymbol{S} & \boldsymbol{I} \\ \boldsymbol{I} & \boldsymbol{R} \end{bmatrix} > 0$$

$$\left[\begin{array}{c|c|c} \boldsymbol{\Psi}_i + \boldsymbol{\Psi}_i^T & \begin{pmatrix} \boldsymbol{B}_1 + \boldsymbol{B}_2\boldsymbol{D}_{ki}\boldsymbol{D}_{21} \\ \boldsymbol{R}\boldsymbol{B}_1 + \boldsymbol{L}_i\boldsymbol{D}_{21} \end{pmatrix} & \begin{pmatrix} \boldsymbol{S}\boldsymbol{C}_1^T + \boldsymbol{F}_i^T\boldsymbol{D}_{12}^T \\ \boldsymbol{C}_1^T + \boldsymbol{C}_2^T\boldsymbol{D}_{ki}^T\boldsymbol{D}_{12}^T \end{pmatrix} \\ \hline \begin{pmatrix} \boldsymbol{B}_1^T + \boldsymbol{D}_{21}^T\boldsymbol{D}_{ki}^T\boldsymbol{B}_2^T & \boldsymbol{B}_1^T\boldsymbol{R} + \boldsymbol{D}_{21}^T\boldsymbol{L}_i^T \end{pmatrix} & -\gamma^2\boldsymbol{I} & \boldsymbol{D}_{11}^T + \boldsymbol{D}_{21}^T\boldsymbol{D}_{ki}^T\boldsymbol{D}_{12}^T \\ \hline \begin{pmatrix} \boldsymbol{C}_1\boldsymbol{S} + \boldsymbol{D}_{12}\boldsymbol{F}_i & \boldsymbol{C}_1 + \boldsymbol{D}_{12}\boldsymbol{D}_{ki}\boldsymbol{C}_2 \end{pmatrix} & \boldsymbol{D}_{11} + \boldsymbol{D}_{12}\boldsymbol{D}_{ki}\boldsymbol{D}_{21} & -\boldsymbol{I} \end{array}\right] < 0, \quad for\ i = 1, \dots, r \tag{12}$$

where $\boldsymbol{\Psi}_i \triangleq \begin{bmatrix} \boldsymbol{A}_i\boldsymbol{S} + \boldsymbol{B}_2\boldsymbol{F}_i & \boldsymbol{A}_i + \boldsymbol{B}_2\boldsymbol{D}_{ki}\boldsymbol{C}_2 \\ \boldsymbol{Q}_i & \boldsymbol{R}\boldsymbol{A}_i + \boldsymbol{L}_i\boldsymbol{C}_2 \end{bmatrix}$, $\boldsymbol{F}_i \triangleq \boldsymbol{D}_{ki}\boldsymbol{C}_2\boldsymbol{S} + \boldsymbol{C}_{ki}\boldsymbol{M}$, $\boldsymbol{L}_i \triangleq \boldsymbol{R}\boldsymbol{B}_2\boldsymbol{D}_{ki} + \boldsymbol{N}^T\boldsymbol{B}_{ki}$, $\boldsymbol{N}^T\boldsymbol{M} = \boldsymbol{I} - \boldsymbol{R}\boldsymbol{S}$, $\boldsymbol{Q}_i \triangleq \boldsymbol{R}\boldsymbol{A}_i\boldsymbol{S} + \boldsymbol{R}\boldsymbol{B}_2\boldsymbol{F}_i + \boldsymbol{N}^T\boldsymbol{B}_{ki}\boldsymbol{C}_2\boldsymbol{S} + \boldsymbol{N}^T\boldsymbol{A}_{ki}\boldsymbol{M}$, with $\boldsymbol{N}$ and $\boldsymbol{M} \in \mathbb{R}^{n\times n}$. The known variables are: $\boldsymbol{A}_i$, $\boldsymbol{B}_1$, $\boldsymbol{B}_2$, $\boldsymbol{C}_1$, $\boldsymbol{C}_2$, $\boldsymbol{D}_{11}$, $\boldsymbol{D}_{12}$, $\boldsymbol{D}_{21}$. The variables obtained through the minimization of γ^2 in Eq. (12) are: $\boldsymbol{D}_{ki}$, $\boldsymbol{F}_i$, $\boldsymbol{L}_i$, $\boldsymbol{Q}_i$, $\boldsymbol{R}$, $\boldsymbol{S}$. The gain-scheduled parameter-dependent controller $\boldsymbol{K}(\theta) = \sum_{i=1}^{r} a_i \left[\begin{array}{c|c} \boldsymbol{A}_{ki} & \boldsymbol{B}_{ki} \\ \hline \boldsymbol{C}_{ki} & \boldsymbol{D}_{ki} \end{array}\right]$ is:

$$\begin{aligned} \boldsymbol{N} &= \boldsymbol{I}_n \\ \boldsymbol{M} &= (\boldsymbol{N}^T)^{-1}(\boldsymbol{I}_n - \boldsymbol{R}\boldsymbol{S}) \\ \boldsymbol{A}_{ki} &= (\boldsymbol{N}^T)^{-1}(\boldsymbol{Q}_i - \boldsymbol{R}\boldsymbol{A}_i\boldsymbol{S} - \boldsymbol{R}\boldsymbol{B}_2\boldsymbol{F}_i - \boldsymbol{N}^T\boldsymbol{B}_{ki}\boldsymbol{C}_2\boldsymbol{S})\boldsymbol{M}^{-1} \\ \boldsymbol{B}_{ki} &= (\boldsymbol{N}^T)^{-1}(\boldsymbol{L}_i - \boldsymbol{R}\boldsymbol{B}_2\boldsymbol{D}_{ki}) \\ \boldsymbol{C}_{ki} &= (\boldsymbol{F}_i - \boldsymbol{D}_{ki}\boldsymbol{C}_2\boldsymbol{S})\boldsymbol{M}^{-1} \\ \boldsymbol{D}_{ki} &= \boldsymbol{D}_{ki} \end{aligned} \qquad for\ i = 1, \dots, r \tag{13}$$

3. PROPOSED METHOD

Although condition (12) can be used in many practical scenarios with the loop-shaping approach, in some cases the LMI-based synthesis tool has difficulty finding a controller that meets the requirements as defined by the weights and reports the problem as infeasible. The very different plant dynamics at the polytope vertices, combined with very strict requirements, can increase this difficulty. Consequently, it is up to the designer to adjust the weights, usually kept the same for all vertices, to comply with the problem requirements and warrant a feasible controller.

To mitigate this difficulty, we propose the weights also be parameter-dependent in a convex polytope (matching the polytopic LPV plant) so that the shaped system dynamics can be individually adjusted at each vertex of the polytope. The goal is to make the open-loop plant (and also the closed-loop) similar in all vertices for the design frequencies. Thus, the LMI-based synthesis tool yields the controller ensuring performance and robustness.

Let state-space realizations of the polytopic LPV plant $\boldsymbol{G}(\theta)$ and weights $\boldsymbol{W}_1$ and $\boldsymbol{W}_2$ used for loop-shaping be

$$\boldsymbol{G}(\theta) \triangleq \left[\begin{array}{c|c} \boldsymbol{A}_G(\theta) & \boldsymbol{B}_G \\ \hline \boldsymbol{C}_G & \boldsymbol{D}_G \end{array}\right] = \sum_{i=1}^{r} a_i \left[\begin{array}{c|c} \boldsymbol{A}_{Gi} & \boldsymbol{B}_G \\ \hline \boldsymbol{C}_G & \boldsymbol{D}_G \end{array}\right] \quad \boldsymbol{W}_1 = \left[\begin{array}{c|c} \boldsymbol{A}_{w1} & \boldsymbol{B}_{w1} \\ \hline \boldsymbol{C}_{w1} & \boldsymbol{D}_{w1} \end{array}\right] \quad \boldsymbol{W}_2 = \left[\begin{array}{c|c} \boldsymbol{A}_{w2} & \boldsymbol{B}_{w2} \\ \hline \boldsymbol{C}_{w2} & \boldsymbol{D}_{w2} \end{array}\right] \tag{14}$$

Consider the notation $\sum_{i=1}^{r} a_i\boldsymbol{A}_i = \sum \boldsymbol{A}_i$. Then, the shaped plant $\boldsymbol{G}_s(\theta)$ in state-space is:

$$\boldsymbol{G}_s(\theta) = \boldsymbol{W}_2\boldsymbol{G}(\theta)\boldsymbol{W}_1 = \left[\begin{array}{ccc|c} \boldsymbol{A}_{w1} & 0 & 0 & \boldsymbol{B}_{w1} \\ \boldsymbol{B}_G\boldsymbol{C}_{w1} & \sum \boldsymbol{A}_{Gi} & 0 & \boldsymbol{B}_G\boldsymbol{D}_{w1} \\ \boldsymbol{B}_{w2}\boldsymbol{D}_G\boldsymbol{C}_{w1} & \boldsymbol{B}_{w2}\boldsymbol{C}_G & \boldsymbol{A}_{w2} & \boldsymbol{B}_{w2}\boldsymbol{D}_G\boldsymbol{D}_{w1} \\ \hline \boldsymbol{D}_{w2}\boldsymbol{D}_G\boldsymbol{C}_{w1} & \boldsymbol{D}_{w2}\boldsymbol{C}_G & \boldsymbol{C}_{w2} & \boldsymbol{D}_{w2}\boldsymbol{D}_G\boldsymbol{D}_{w1} \end{array}\right] = \sum_{i=1}^{r} a_i \left[\begin{array}{c|c} \boldsymbol{A}_{GSi} & \boldsymbol{B}_{GS} \\ \hline \boldsymbol{C}_{GS} & \boldsymbol{D}_{GS} \end{array}\right] \tag{15}$$

Note that only matrix $\boldsymbol{A}_{GS}(\theta)$ is parameter-dependent. The final controller $\boldsymbol{K}_F(\theta)$ in state-space is:

$$\boldsymbol{K}_F(\theta) = \boldsymbol{W}_1\boldsymbol{K}(\theta)\boldsymbol{W}_2 = \left[\begin{array}{ccc|c} \boldsymbol{A}_{w2} & 0 & 0 & \boldsymbol{B}_{w2} \\ \sum \boldsymbol{B}_{ki}\boldsymbol{C}_{w2} & \sum \boldsymbol{A}_{ki} & 0 & \sum \boldsymbol{B}_{ki}\boldsymbol{D}_{w2} \\ \boldsymbol{B}_{w1}\sum \boldsymbol{D}_{ki}\boldsymbol{C}_{w2} & \boldsymbol{B}_{w1}\sum \boldsymbol{C}_{ki} & \boldsymbol{A}_{w1} & \boldsymbol{B}_{w1}\sum \boldsymbol{D}_{ki}\boldsymbol{D}_{w2} \\ \hline \boldsymbol{D}_{w1}\sum \boldsymbol{D}_{ki}\boldsymbol{C}_{w2} & \boldsymbol{D}_{w1}\sum \boldsymbol{C}_{ki} & \boldsymbol{C}_{w1} & \boldsymbol{D}_{w1}\sum \boldsymbol{D}_{ki}\boldsymbol{D}_{w2} \end{array}\right] = \sum_{i=1}^{r} a_i \left[\begin{array}{c|c} \boldsymbol{A}_{KFi} & \boldsymbol{B}_{KFi} \\ \hline \boldsymbol{C}_{KFi} & \boldsymbol{D}_{KFi} \end{array}\right] \tag{16}$$

Define now the weights also as parameter-dependent in a convex polytope:

$$\boldsymbol{W}_1(\theta) \triangleq \sum_{i=1}^{r} a_i \left[\begin{array}{c|c} \boldsymbol{A}_{w1i} & \boldsymbol{B}_{w1i} \\ \hline \boldsymbol{C}_{w1i} & \boldsymbol{D}_{w1i} \end{array}\right] \qquad \boldsymbol{W}_2(\theta) \triangleq \sum_{i=1}^{r} a_i \left[\begin{array}{c|c} \boldsymbol{A}_{w2i} & \boldsymbol{B}_{w2i} \\ \hline \boldsymbol{C}_{w2i} & \boldsymbol{D}_{w2i} \end{array}\right] \tag{17}$$

Now, the shaped plant $\boldsymbol{G}_s(\theta)$ in state-space is:

$$\boldsymbol{G}_s(\theta) = \boldsymbol{W}_2(\theta)\boldsymbol{G}(\theta)\boldsymbol{W}_1(\theta) = \left[\begin{array}{ccc|c} \sum \boldsymbol{A}_{w1i} & 0 & 0 & \sum \boldsymbol{B}_{w1i} \\ \boldsymbol{B}_G \sum \boldsymbol{C}_{w1i} & \sum \boldsymbol{A}_{Gi} & 0 & \boldsymbol{B}_G \sum \boldsymbol{D}_{w1i} \\ \sum \boldsymbol{B}_{w2i}\boldsymbol{D}_G \sum \boldsymbol{C}_{w1i} & \sum \boldsymbol{B}_{w2i}\boldsymbol{C}_G & \sum \boldsymbol{A}_{w2i} & \sum \boldsymbol{B}_{w2i}\boldsymbol{D}_G \sum \boldsymbol{D}_{w1i} \\ \hline \sum \boldsymbol{D}_{w2i}\boldsymbol{D}_G \sum \boldsymbol{C}_{w1i} & \sum \boldsymbol{D}_{w2i}\boldsymbol{C}_G & \sum \boldsymbol{C}_{w2i} & \sum \boldsymbol{D}_{w2i}\boldsymbol{D}_G \sum \boldsymbol{D}_{w1i} \end{array}\right] \tag{18}$$

but this description of $\boldsymbol{G}_s(\theta)$ cannot be used directly to obtain the H_∞ controller via LMI in Eq. (12) because the generalized plant associated with $\boldsymbol{G}_s(\theta)$ violates the polytopic description of Eq. (11). Assuming

$$\boldsymbol{G}(\theta) \triangleq \sum_{i=1}^{r} a_i \left[\begin{array}{c|c} \boldsymbol{A}_{Gi} & \boldsymbol{B}_G \\ \hline \boldsymbol{C}_G & 0 \end{array}\right] \tag{19}$$

this paper proposes two configurations for $\boldsymbol{W}_1(\theta)$ and $\boldsymbol{W}_2(\theta)$ that warrant the synthesis of the output feedback dynamic H_∞ controller via loop-shaping approach: (i) $\boldsymbol{W}_1(\theta)$ and $\boldsymbol{W}_2(\theta)$ partially parameter-dependent, and (ii) $\boldsymbol{W}_1(\theta)$ and $\boldsymbol{W}_2(\theta)$ totally parameter-dependent. The use of either one will depend on the loop-shaping requirements of the problem. In the first, only two matrices of the state-space description of the weights can be parameter-dependent but the stabilizing controller $\boldsymbol{K}(\theta)$ is free to have all the four matrices parameter-dependent. In the second, the stabilizing controller $\boldsymbol{K}(\theta)$ is limited to has only matrix $\boldsymbol{A}_k(\theta)$ as parameter-dependent and $\boldsymbol{D}_k = 0$ but the weights are free to have all the four matrices parameter-dependent. The polytopic LPV plant $\boldsymbol{G}(\theta)$ is required to be in the form of the equation (19). To this end, the plant $\boldsymbol{G}(\theta)$ can be augmented with the sensors and actuators used in the control design. An alternative is the use of filters to move the parameter dependence to the matrix $\boldsymbol{A}$, as suggested in Apkarian and Gahinet (1995a).

3.1 $\mathbf{W}_1(\theta)$ and $\mathbf{W}_2(\theta)$ partially parameter-dependent

Theorem 1 *If* $\boldsymbol{W}_1(\theta) \triangleq \sum_{i=1}^{r} a_i \left[\begin{array}{c|c} \boldsymbol{A}_{w1i} & \boldsymbol{B}_{w1} \\ \hline \boldsymbol{C}_{w1i} & \boldsymbol{D}_{w1} \end{array}\right]$ *and* $\boldsymbol{W}_2(\theta) \triangleq \sum_{i=1}^{r} a_i \left[\begin{array}{c|c} \boldsymbol{A}_{w2i} & \boldsymbol{B}_{w2i} \\ \hline \boldsymbol{C}_{w2} & \boldsymbol{D}_{w2} \end{array}\right]$ *are partially parameter-dependent, then it is possible to find an output feedback dynamic* H_∞ *controller* $\boldsymbol{K}_F(\theta)$ *using four-block loop-shaping with* $\boldsymbol{K}(\theta) = \sum_{i=1}^{r} a_i \left[\begin{array}{c|c} \boldsymbol{A}_{ki} & \boldsymbol{B}_{ki} \\ \hline \boldsymbol{C}_{ki} & \boldsymbol{D}_{ki} \end{array}\right]$ *resulting directly from Eqs. (12) and (13).*

Proof. Using the defined weights and the assumption of Eq. (19) in Eq. (18) we have:

$$\boldsymbol{G}_s(\theta) = \boldsymbol{W}_2(\theta)\boldsymbol{G}(\theta)\boldsymbol{W}_1(\theta) = \sum_{i=1}^{r} a_i \left[\begin{array}{ccc|c} \boldsymbol{A}_{w1i} & 0 & 0 & \boldsymbol{B}_{w1} \\ \boldsymbol{B}_G\boldsymbol{C}_{w1i} & \boldsymbol{A}_{Gi} & 0 & \boldsymbol{B}_G\boldsymbol{D}_{w1} \\ 0 & \boldsymbol{B}_{w2i}\boldsymbol{C}_G & \boldsymbol{A}_{w2i} & 0 \\ \hline 0 & \boldsymbol{D}_{w2}\boldsymbol{C}_G & \boldsymbol{C}_{w2} & 0 \end{array}\right] = \sum_{i=1}^{r} a_i \left[\begin{array}{c|c} \boldsymbol{A}_{GSi} & \boldsymbol{B}_{GS} \\ \hline \boldsymbol{C}_{GS} & 0 \end{array}\right] \tag{20}$$

Note that in $\boldsymbol{G}_s(\theta)$ only matrix $\boldsymbol{A}_{GS}(\theta)$ is parameter-dependent. Therefore, $\boldsymbol{G}_s(\theta)$ can be described as the generalized plant in Eq. (11) using Eq. (5), and Eq. (12) holds. Using Eq. (13), we obtain $\boldsymbol{K}(\theta)$ and the final loop-shaping controller derives from the defined weights:

$$\boldsymbol{K}_F(\theta) = \boldsymbol{W}_1(\theta)\boldsymbol{K}(\theta)\boldsymbol{W}_2(\theta) = \sum_{i=1}^{r} a_i \left[\begin{array}{ccc|c} \boldsymbol{A}_{w2i} & 0 & 0 & \boldsymbol{B}_{w2i} \\ \boldsymbol{B}_{ki}\boldsymbol{C}_{w2} & \boldsymbol{A}_{ki} & 0 & \boldsymbol{B}_{ki}\boldsymbol{D}_{w2} \\ \boldsymbol{B}_{w1}\boldsymbol{D}_{ki}\boldsymbol{C}_{w2} & \boldsymbol{B}_{w1}\boldsymbol{C}_{ki} & \boldsymbol{A}_{w1i} & \boldsymbol{B}_{w1}\boldsymbol{D}_{ki}\boldsymbol{D}_{w2} \\ \hline \boldsymbol{D}_{w1}\boldsymbol{D}_{ki}\boldsymbol{C}_{w2} & \boldsymbol{D}_{w1}\boldsymbol{C}_{ki} & \boldsymbol{C}_{w1i} & \boldsymbol{D}_{w1}\boldsymbol{D}_{ki}\boldsymbol{D}_{w2} \end{array}\right] = \sum_{i=1}^{r} a_i \left[\begin{array}{c|c} \boldsymbol{A}_{KFi} & \boldsymbol{B}_{KFi} \\ \hline \boldsymbol{C}_{KFi} & \boldsymbol{D}_{KFi} \end{array}\right] \tag{21}$$

and, surely, is described in a polytopic form.□

3.2 $\mathbf{W}_1(\theta)$ and $\mathbf{W}_2(\theta)$ totally parameter-dependent

Theorem 2 *Let the generalized plant be in the form*

$$\boldsymbol{P}(\theta) \triangleq \left[\begin{array}{c|cc} \boldsymbol{A}(\theta) & \boldsymbol{B}_1(\theta) & \boldsymbol{B}_2(\theta) \\ \hline \boldsymbol{C}_1(\theta) & \boldsymbol{D}_{11}(\theta) & \boldsymbol{D}_{12}(\theta) \\ \boldsymbol{C}_2(\theta) & \boldsymbol{D}_{21}(\theta) & \boldsymbol{D}_{22}(\theta)=0 \end{array}\right] = \sum_{i=1}^{r} a_i \left[\begin{array}{c|cc} \boldsymbol{A}_i & \boldsymbol{B}_{1i} & \boldsymbol{B}_{2i} \\ \hline \boldsymbol{C}_{1i} & \boldsymbol{D}_{11i} & \boldsymbol{D}_{12i} \\ \boldsymbol{C}_{2i} & \boldsymbol{D}_{21i} & 0 \end{array}\right] \tag{22}$$

Then it is possible to synthesize an output feedback dynamic H_∞ controller $\boldsymbol{K}(\theta)$ if we define

$$\boldsymbol{K}(\theta) \triangleq \left[\begin{array}{c|c} \boldsymbol{A}_k(\theta) & \boldsymbol{B}_k \\ \hline \boldsymbol{C}_k & \boldsymbol{D}_k=0 \end{array}\right] = \sum_{i=1}^{r} a_i \left[\begin{array}{c|c} \boldsymbol{A}_{ki} & \boldsymbol{B}_k \\ \hline \boldsymbol{C}_k & 0 \end{array}\right] \tag{23}$$

in Eq. (12) with $\boldsymbol{D}_k = 0$ and only matrix $\boldsymbol{A}_k(\theta)$ as parameter-dependent.

Proof. Let us consider the generalized plant of Eq. (22) and the controller of Eq. (23), both subject to the condition in Eq. (12). Then we have the new condition without incurring in any convexity problem in the synthesis:

$$\begin{bmatrix} \boldsymbol{S} & \boldsymbol{I} \\ \boldsymbol{I} & \boldsymbol{R} \end{bmatrix} > 0$$
$$\left[\begin{array}{c|c|c} \boldsymbol{\Psi}_i + \boldsymbol{\Psi}_i^T & \begin{pmatrix} \boldsymbol{B}_{1i} \\ \boldsymbol{R}\boldsymbol{B}_{1i} + \boldsymbol{L}\boldsymbol{D}_{21i} \end{pmatrix} & \begin{pmatrix} \boldsymbol{S}\boldsymbol{C}_{1i}^T + \boldsymbol{F}^T\boldsymbol{D}_{12i}^T \\ \boldsymbol{C}_{1i}^T \end{pmatrix} \\ \hline \begin{pmatrix} \boldsymbol{B}_{1i}^T & \boldsymbol{B}_{1i}^T\boldsymbol{R} + \boldsymbol{D}_{21i}^T\boldsymbol{L}^T \end{pmatrix} & -\gamma^2\boldsymbol{I} & \boldsymbol{D}_{11i}^T \\ \hline \begin{pmatrix} \boldsymbol{C}_{1i}\boldsymbol{S} + \boldsymbol{D}_{12i}\boldsymbol{F} & \boldsymbol{C}_{1i} \end{pmatrix} & \boldsymbol{D}_{11i} & -\boldsymbol{I} \end{array}\right] < 0, \quad for\ i = 1, \ldots, r \tag{24}$$

where $\boldsymbol{\Psi}_i = \begin{bmatrix} \boldsymbol{A}_i\boldsymbol{S} + \boldsymbol{B}_{2i}\boldsymbol{F} & \boldsymbol{A}_i \\ \boldsymbol{Q}_i & \boldsymbol{R}\boldsymbol{A}_i + \boldsymbol{L}\boldsymbol{C}_{2i} \end{bmatrix}$, $\boldsymbol{F} = \boldsymbol{C}_k\boldsymbol{M}$, $\boldsymbol{L} = \boldsymbol{N}^T\boldsymbol{B}_k$, $\boldsymbol{N}^T\boldsymbol{M} = \boldsymbol{I} - \boldsymbol{R}\boldsymbol{S}$, $\boldsymbol{Q}_i = \boldsymbol{R}\boldsymbol{A}_i\boldsymbol{S} + \boldsymbol{R}\boldsymbol{B}_{2i}\boldsymbol{F} + \boldsymbol{N}^T\boldsymbol{B}_k\boldsymbol{C}_{2i}\boldsymbol{S} + \boldsymbol{N}^T\boldsymbol{A}_{ki}\boldsymbol{M}$. The known variables are: $\boldsymbol{A}_i$, $\boldsymbol{B}_{1i}$, $\boldsymbol{B}_{2i}$, $\boldsymbol{C}_{1i}$, $\boldsymbol{C}_{2i}$, $\boldsymbol{D}_{11i}$, $\boldsymbol{D}_{12i}$, $\boldsymbol{D}_{21i}$. The variables obtained through the minimization of γ^2 in Eq. (24) are: $\boldsymbol{F}$, $\boldsymbol{L}$, $\boldsymbol{Q}_i$, $\boldsymbol{R} = \boldsymbol{R}^T$, $\boldsymbol{S} = \boldsymbol{S}^T$. Similarly to Eq. (13), the gain-scheduled parameter-dependent controller $\boldsymbol{K}(\theta)$ is:

$$\begin{aligned} \boldsymbol{N} &= \boldsymbol{I}_n \\ \boldsymbol{M} &= (\boldsymbol{N}^T)^{-1}(\boldsymbol{I}_n - \boldsymbol{R}\boldsymbol{S}) \\ \boldsymbol{A}_{ki} &= (\boldsymbol{N}^T)^{-1}(\boldsymbol{Q}_i - \boldsymbol{R}\boldsymbol{A}_i\boldsymbol{S} - \boldsymbol{R}\boldsymbol{B}_{2i}\boldsymbol{F} - \boldsymbol{N}^T\boldsymbol{B}_k\boldsymbol{C}_{2i}\boldsymbol{S})\boldsymbol{M}^{-1} \\ \boldsymbol{B}_k &= (\boldsymbol{N}^T)^{-1}\boldsymbol{L} \\ \boldsymbol{C}_k &= \boldsymbol{F}\boldsymbol{M}^{-1} \\ \boldsymbol{D}_k &= 0 \end{aligned} \qquad for\ i = 1, \ldots, r \tag{25}$$

□

Theorem 3 *If $\boldsymbol{W}_1(\theta) \triangleq \sum_{i=1}^{r} a_i \left[\begin{array}{c|c} \boldsymbol{A}_{w1i} & \boldsymbol{B}_{w1i} \\ \hline \boldsymbol{C}_{w1i} & \boldsymbol{D}_{w1i} \end{array}\right]$ and $\boldsymbol{W}_2(\theta) \triangleq \sum_{i=1}^{r} a_i \left[\begin{array}{c|c} \boldsymbol{A}_{w2i} & \boldsymbol{B}_{w2i} \\ \hline \boldsymbol{C}_{w2i} & \boldsymbol{D}_{w2i} \end{array}\right]$ are totally parameter-dependent, then it is possible to find an output feedback dynamic H_∞ controller $\boldsymbol{K}_F(\theta)$ using four-block loop-shaping if we define $\boldsymbol{K}(\theta) \triangleq \sum_{i=1}^{r} a_i \left[\begin{array}{c|c} \boldsymbol{A}_{ki} & \boldsymbol{B}_k \\ \hline \boldsymbol{C}_k & 0 \end{array}\right]$ as in Eq. (23).*

Proof. Using the defined weights and the assumption of Eq. (19) in Eq. (18) we have:

$$\boldsymbol{G}_s(\theta) = \boldsymbol{W}_2(\theta)\boldsymbol{G}(\theta)\boldsymbol{W}_1(\theta) = \sum_{i=1}^{r} a_i \left[\begin{array}{ccc|c} \boldsymbol{A}_{w1i} & 0 & 0 & \boldsymbol{B}_{w1i} \\ \boldsymbol{B}_G\boldsymbol{C}_{w1i} & \boldsymbol{A}_{Gi} & 0 & \boldsymbol{B}_G\boldsymbol{D}_{w1i} \\ 0 & \boldsymbol{B}_{w2i}\boldsymbol{C}_G & \boldsymbol{A}_{w2i} & 0 \\ \hline 0 & \boldsymbol{D}_{w2i}\boldsymbol{C}_G & \boldsymbol{C}_{w2i} & 0 \end{array}\right] = \sum_{i=1}^{r} a_i \left[\begin{array}{c|c} \boldsymbol{A}_{GSi} & \boldsymbol{B}_{GSi} \\ \hline \boldsymbol{C}_{GSi} & 0 \end{array}\right] \tag{26}$$

Note that $\boldsymbol{G}_s(\theta)$ can be described as the generalized plant in Eq. (22) using Eq. (5). By Theorem 2, we obtain the stabilizing controller $\boldsymbol{K}(\theta)$. The final loop-shaping controller derives from the defined weights and Eq. (23):

$$\boldsymbol{K}_F(\theta) = \boldsymbol{W}_1(\theta)\boldsymbol{K}(\theta)\boldsymbol{W}_2(\theta) = \sum_{i=1}^{r} a_i \left[\begin{array}{ccc|c} \boldsymbol{A}_{w2i} & 0 & 0 & \boldsymbol{B}_{w2i} \\ \boldsymbol{B}_k\boldsymbol{C}_{w2i} & \boldsymbol{A}_{ki} & 0 & \boldsymbol{B}_k\boldsymbol{D}_{w2i} \\ 0 & \boldsymbol{B}_{w1i}\boldsymbol{C}_k & \boldsymbol{A}_{w1i} & 0 \\ \hline 0 & \boldsymbol{D}_{w1i}\boldsymbol{C}_k & \boldsymbol{C}_{w1i} & 0 \end{array}\right] = \sum_{i=1}^{r} a_i \left[\begin{array}{c|c} \boldsymbol{A}_{KFi} & \boldsymbol{B}_{KFi} \\ \hline \boldsymbol{C}_{KFi} & 0 \end{array}\right] \tag{27}$$

and, surely, is described in a polytopic form.□

4. MISSILE MODEL

The missile used as SAM in this paper and its aerodynamic model were taken from Evangelista (2019) and adapted for this work. The aerodynamic coefficients and their derivatives were obtained for angle-of-attack α and Mach number between $-20^o < \alpha < 20^o$ and $0 < Mach < 4$ at sea level. For the longitudinal model of the missile, all coefficients are nonlinear functions of α and Mach, with sideslip angle $\beta = 0$. The derivatives as a function of other variables (β, pitch rate q, and others) are obtained by inserting small perturbations (Blake, 1998).

For the nonlinear simulation, the nonlinear missile model was implemented in Matlab. The 6-degree-of-freedom simulation of the skid-to-turn missile has proportional navigation as guidance law. We are interested in the end game, when the missile pursues the target using its own seeker. The entire rocket motor has been consumed and there are no variations in mass, center of gravity or moment of inertia. The actuator and seeker were both first-order transfer functions:

$$\frac{\delta}{\delta_{com}} = \frac{1}{\tau_{ac}s+1}, \;\; \tau_{ac} = 0.05\ s, \qquad and \qquad \frac{\dot{\lambda}_{sk}}{\dot{\lambda}} = \frac{1}{\tau_{sk}s+1}, \;\; \tau_{sk} = 0.01\ s \tag{28}$$

where $\dot{\lambda}$ is the line-of-sight rate from missile to target, $\dot{\lambda}_{sk}$ is the line-of-sight rate measured by the seeker, δ is the actual actuator deflection and δ_{com} is the commanded actuator deflection by the autopilot. The maximum actuator deflection was assumed as 10^o.

According to Apkarian and Gahinet (1995a), three variables define the flight conditions (also called operation point): angle-of-attack, airspeed and altitude. Assuming there is no wind, airspeed equals the missile ground speed. For design purposes, it is necessary to describe the missile model depending on the measured parameter vector $\theta(t)$ and we assume that the missile is symmetrical with pitch, yaw and roll axes decoupled. We develop only the longitudinal model (the lateral one is equivalent). Considering constant the missile speed, without aerodynamic drag, and defining the following variables as α (angle-of-attack) parameter-dependent:

$$Z_\alpha(\alpha) \triangleq \frac{Q_{din}.S_{ref}.C_{za}(\alpha)}{m.V_{tot}} \qquad Z_q(\alpha) \triangleq 1 + \frac{Q_{din}.S_{ref}.d_{ref}.C_{zq}(\alpha)}{2.m.V_{tot}^2} \qquad Z_\delta(\alpha) \triangleq \frac{Q_{din}.S_{ref}.C_{z\delta}(\alpha)}{m.V_{tot}} \tag{29}$$

$$M_\alpha(\alpha) \triangleq \frac{Q_{din}.S_{ref}.d_{ref}.C_{ma}(\alpha)}{I_y} \qquad M_q(\alpha) \triangleq \frac{Q_{din}.S_{ref}.d_{ref}^2.C_{mq}(\alpha)}{2.I_y.V_{tot}} \qquad M_\delta(\alpha) \triangleq \frac{Q_{din}.S_{ref}.d_{ref}.C_{m\delta}(\alpha)}{I_y} \tag{30}$$

where $Q_{din} = 0.5\rho V_{tot}^2$ is the dynamic pressure, ρ is the air density, V_{tot} is the missile speed, m is the mass of the missile, I_y is the moment about body y axis, S_{ref} is the reference area of the missile, d_{ref} is the reference length of the missile, and $C_{za},\ C_{zq},\ C_{z\delta},\ C_{ma},\ C_{mq},\ C_{m\delta},$ are aerodynamics coefficients, the longitudinal parameter-dependent missile model in state-space is:

$$\begin{aligned} \begin{bmatrix}\dot{\alpha}\\ \dot{q}\end{bmatrix} &= \begin{bmatrix} Z_\alpha(\alpha) & Z_q(\alpha) \\ M_\alpha(\alpha) & M_q(\alpha)\end{bmatrix}\begin{bmatrix}\alpha\\ q\end{bmatrix} + \begin{bmatrix} Z_\delta(\alpha) \\ M_\delta(\alpha)\end{bmatrix}\delta_p \\ a_{mz} &= \begin{bmatrix} V_{tot}Z_\alpha(\alpha) & V_{tot}.Z_q(\alpha) - V_{tot}\end{bmatrix}\begin{bmatrix}\alpha\\ q\end{bmatrix} + \begin{bmatrix} V_{tot}.Z_\delta(\alpha)\end{bmatrix}\delta_p \end{aligned} \tag{31}$$

where angle-of-attack α and pitch rate q are states, δ_p is the pitch actuator and the output is the missile acceleration a_{mz} in the body z axis. The aerodynamics coefficients vary little with Mach number in the range $2 < Mach < 4$. Then, we focus on this range to develop the controller because a surface-to-air missile will not operate at low speeds. Establishing a sea level scenario at Mach 3, variables Z_δ, Z_q and M_q are almost constants and the model is:

$$\begin{aligned} \begin{bmatrix}\dot{\alpha}\\ \dot{q}\end{bmatrix} &= \begin{bmatrix} -0.01M_\alpha(\alpha) - 5.75 & 1 \\ M_\alpha(\alpha) & -2.8\end{bmatrix}\begin{bmatrix}\alpha\\ q\end{bmatrix} + \begin{bmatrix} -0.2 \\ M_\delta(\alpha)\end{bmatrix}\delta_p \\ a_{mz} &= \begin{bmatrix} 1020.8(-0.01M_\alpha(\alpha) - 5.75) & 0\end{bmatrix}\begin{bmatrix}\alpha\\ q\end{bmatrix} + \begin{bmatrix} -204.2\end{bmatrix}\delta_p \end{aligned} \tag{32}$$

with the parameters $M_\alpha(\alpha)$ and $M_\delta(\alpha)$ registered in Figures 3 and 4. Note that the model has two time-varying parameters $M_\alpha(\alpha(t))$ and $M_\delta(\alpha(t))$ depend on the single time-varying angle-of-attack parameter $\alpha(t)$, which we assume that can be measured. The time-varying parameters vector is defined as $\theta(t) = \begin{bmatrix} M_\delta(\alpha(t)) & M_\alpha(\alpha(t))\end{bmatrix}^T$. That is, the open-loop transfer function has the form

$$\begin{aligned} &\begin{bmatrix} \boldsymbol{A}(\theta) & \boldsymbol{B}(\theta) \\ \boldsymbol{C}(\theta) & \boldsymbol{D}\end{bmatrix} \in Co\left\{\begin{bmatrix} \boldsymbol{A}_i & \boldsymbol{B}_i \\ \boldsymbol{C}_i & \boldsymbol{D}\end{bmatrix} \triangleq \begin{bmatrix} \boldsymbol{A}(\xi_i) & \boldsymbol{B}(\xi_i) \\ \boldsymbol{C}(\xi_i) & \boldsymbol{D}\end{bmatrix}\right\},\ i = 1,\ \ldots, 4 \\ &\theta(t) \in \Theta \triangleq \left\{\textstyle\sum_{i=1}^4 a_i\xi_i,\ a_i \geq 0,\ \sum_{i=1}^4 a_i = 1\right\} \end{aligned} \tag{33}$$

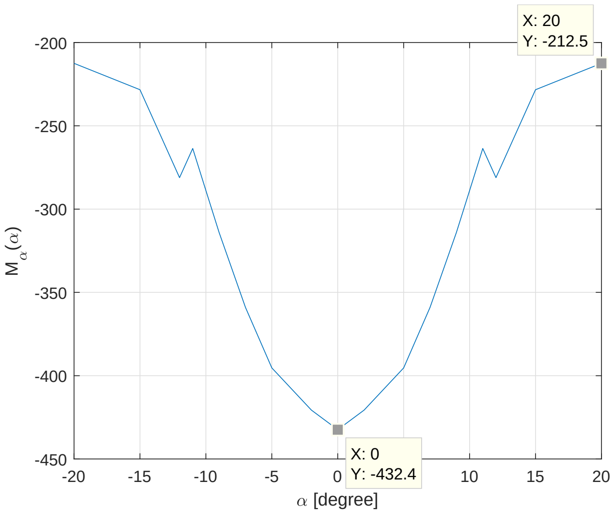

Figure 3. Time-varying parameter $M_\alpha(\alpha)$ for Mach 3.

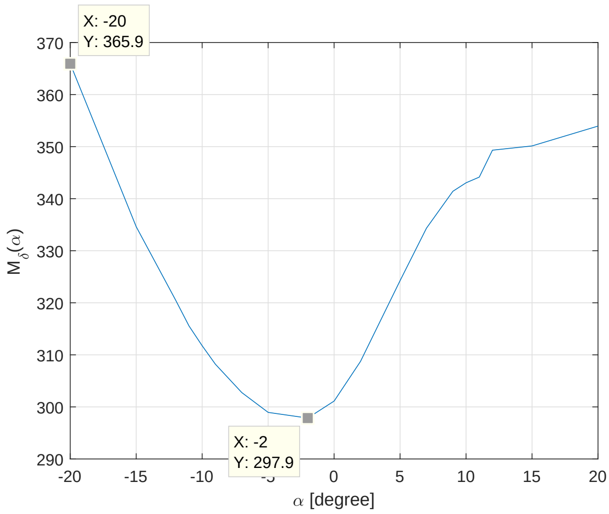

Figure 4. Time-varying parameter $M_\delta(\alpha)$ for Mach 3.

with the following polytope vertices ξ_i and coordinates a_i:

$$\begin{aligned}
\xi_1 &\triangleq \begin{bmatrix} M_\delta^{min} & M_\alpha^{min} \end{bmatrix} = \begin{bmatrix} 297.9 & -432.4 \end{bmatrix} & a_1 &= \frac{M_\delta^{max} - M_\delta(\alpha(t))}{M_\delta^{max} - M_\delta^{min}} \left(1 - \frac{M_\alpha(\alpha(t)) - M_\alpha^{min}}{M_\alpha^{max} - M_\alpha^{min}} \right) \\
\xi_2 &\triangleq \begin{bmatrix} M_\delta^{min} & M_\alpha^{max} \end{bmatrix} = \begin{bmatrix} 297.9 & -212.5 \end{bmatrix} & a_2 &= \frac{M_\delta^{max} - M_\delta(\alpha(t))}{M_\delta^{max} - M_\delta^{min}} \left(\frac{M_\alpha(\alpha(t)) - M_\alpha^{min}}{M_\alpha^{max} - M_\alpha^{min}} \right) \\
\xi_3 &\triangleq \begin{bmatrix} M_\delta^{max} & M_\alpha^{min} \end{bmatrix} = \begin{bmatrix} 365.9 & -432.4 \end{bmatrix} & a_3 &= \left(1 - \frac{M_\delta^{max} - M_\delta(\alpha(t))}{M_\delta^{max} - M_\delta^{min}} \right) \left(1 - \frac{M_\alpha(\alpha(t)) - M_\alpha^{min}}{M_\alpha^{max} - M_\alpha^{min}} \right) \\
\xi_4 &\triangleq \begin{bmatrix} M_\delta^{max} & M_\alpha^{max} \end{bmatrix} = \begin{bmatrix} 365.9 & -212.5) \end{bmatrix} & a_4 &= \left(1 - \frac{M_\delta^{max} - M_\delta(\alpha(t))}{M_\delta^{max} - M_\delta^{min}} \right) \frac{M_\alpha(\alpha(t)) - M_\alpha^{min}}{M_\alpha^{max} - M_\alpha^{min}}
\end{aligned} \tag{34}$$

5. DESIGN RESULTS AND DISCUSSIONS

The LPV plant of Eq. (32) and (33) is a simplified model of the longitudinal dynamics of the missile. It is a polytopic representation and has four vertices. The output is the missile acceleration in body z axis and the input is the pitch actuator deflection. The goal of the autopilot is to track the guidance law acceleration reference proportional to the target-missile line-of-sight rate measured by the seeker.

The output is measured by an ideal accelerometer. The shorter the delay between reference and output the smaller will be the miss distance between the missile and the target. To achieve this, we use the output feedback dynamic H_∞ controller associated with the four-block loop-shaping approach. In addition to minimizing the output error, this approach also minimizes the control signal. As the missile was assumed symmetrical, the longitudinal design was also used for the lateral autopilot.

The following output requirements have been established for the close-loop system: steady state error less than 10%, rise time less than 0.3 s, settling time less than 1 s and actuator deflections between -10 and 10 degrees. For the design with loop-shaping, the longitudinal model in Eq. (32) is augmented with the actuator dynamics in Eq. (28) and a filter to obtain the plant $\boldsymbol{G}(\theta)$ in the form of Eq. (19). The first-order low-pass filter with a time constant of 0.001 second is used just for design. Then, the plant $\boldsymbol{G}(\theta)$ has 4 states and is shaped using the weights to obtain $\boldsymbol{G}_s(\theta)$, according to Eq. (20). As we achieve the design requirements using the weights partially parameter-dependent, we use the strategy proposed in section 3.1 enabling the stabilizing controller $\boldsymbol{K}(\theta)$ to be completely described in a polytopic form. Using this strategy, we independently tune the weights for each vertex of the polytopic LPV plant.

We choose the weight $\boldsymbol{W}_1(\theta)$ as a first order low-pass filter in the form $\dfrac{1}{\eta s + 1}$ defined in state-space as:

$$\boldsymbol{W}_1(\theta) = \sum_{i=1}^{r} a_i \boldsymbol{W}_{1(i)} = \sum_{i=1}^{r} a_i \left[\begin{array}{c|c} \boldsymbol{A}_{w1i} & \boldsymbol{B}_{w1} \\ \hline \boldsymbol{C}_{w1i} & \boldsymbol{D}_{w1} \end{array} \right] = \sum_{i=1}^{r} a_i \left[\begin{array}{c|c} -\eta_i & 1 \\ \hline \eta_i & 0 \end{array} \right] \tag{35}$$

where η_i are the parameters to be set. The weight $\boldsymbol{W}_2(\theta)$ has the form of a PI filter $\dfrac{\zeta s + \mu}{s}$ and behaves like an integrator at DC. It can be described in state-space as:

$$\boldsymbol{W}_2(\theta) = \sum_{i=1}^{r} a_i \boldsymbol{W}_{2(i)} = \sum_{i=1}^{r} a_i \left[\begin{array}{c|c} \boldsymbol{A}_{w2} & \boldsymbol{B}_{w2i} \\ \hline \boldsymbol{C}_{w2} & \boldsymbol{D}_{w2} \end{array} \right] = \sum_{i=1}^{r} a_i \left[\begin{array}{c|c} 0 & \zeta_i \\ \hline 1 & \mu \end{array} \right] \tag{36}$$

where ζ_i and μ are the parameters to be defined. Note that μ does not change at the i^{th} vertex.

The weights' parameters are tuned with a trial-and-error procedure: the behavior of the open-loop system $\boldsymbol{G}_s(\theta)$ is inspected at all the polytope vertices and the weights are adjusted. At this point, note that $\boldsymbol{G}_s(\theta)$ has 6 states. Sequentially, condition (12) and (13) are used to find the controller $\boldsymbol{K}(\theta)$ for the parameters previously set. Then, the final controller $\boldsymbol{K}_F(\theta)$ is computed as in Eq. (21). Thereafter, the behavior of the closed-loop plant is verified at the vertices. This process is repeated until the requirements are met and the control signal is minimized. The final values tuned for the weights are the following:

$$\boldsymbol{W}_{1(i)} = \left[\begin{array}{c|c} -300 & 1 \\ \hline 300 & 0 \end{array}\right] \qquad \boldsymbol{W}_{2(1)} = \boldsymbol{W}_{2(3)} = \left[\begin{array}{c|c} 0 & 0.05 \\ \hline 1 & 0.001 \end{array}\right] \qquad \boldsymbol{W}_{2(2)} = \boldsymbol{W}_{2(4)} = \left[\begin{array}{c|c} 0 & 0.01 \\ \hline 1 & 0.001 \end{array}\right] \tag{37}$$

Figure 5 shows the singular values for shaped (in red) and non-shaped (in blue) plants, with four vertices for each. Note that the behavior of the shaped plant is identical for all four vertices, at frequencies less than 10 rad/s (low frequencies). The same happens at frequencies above than 200 rad/s (high frequencies). Such result could only be achieved by using the proposed loop-shaping with parameter-dependent weights. The final loop-shaping controller $\boldsymbol{K}_F(\theta)$ is a four-vertex

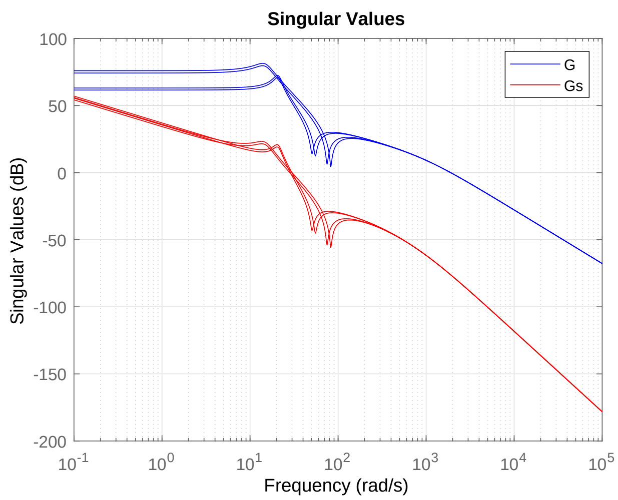

Figure 5. Singular values for all four vertices of the $G(\theta)$ and $G_s(\theta)$.

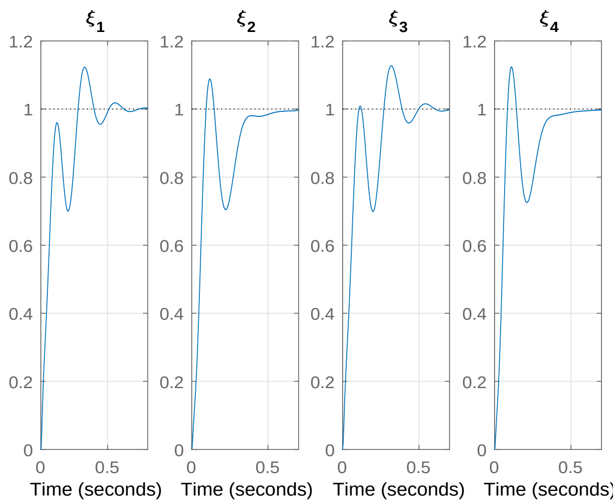

Figure 6. Step responses for closed-loop in all four vertices (order reduced).

polytope, eighth-order controller. The achieved norm H_∞ for the closed-loop system is $\|F_l(\boldsymbol{G}(\theta), \boldsymbol{K}_F(\theta))\|_\infty = 5.7$.

The autopilot design was tested with a 6-degree-of-freedom nonlinear simulation. The nonlinear missile model was implemented in Matlab. Despite the fact that the controller achieved the requirements, non-linear simulations were very slow. Then, we implemented a controller order reduction, eliminating the 3 fastest poles. The new $\boldsymbol{K}_{red}(\theta)$ had order 5, 4 vertices, and also achieved the performance requirements. Figure 6 registers the step response of the closed-loop system for all vertices. The parameter-dependent controller $\boldsymbol{K}_{red}(\theta)$ is used in both longitudinal and lateral autopilots. The aerodynamic coefficients are nonlinear and dependent on measuring α (or β) and Mach number. The integration method used is Runge-Kutta 4^{th} order with a fixed step of 10^{-3} second.

The simulation emulates engagements against a subsonic aircraft or an anti-surface missile. The target speed is approximately Mach 0.8. The initial missile speed is Mach 3 at a sea-level flight, with aerodynamic drag, flat earth model as an inertial frame of reference, and no wind. The target tries to evade with a 3-g random maneuver (without changing magnitude speed). We define in the inertial reference frame the initial missile position as $\boldsymbol{P}_{m0} = [0\ 0\ 0]^T$ and initial target velocity $\boldsymbol{V}_{t0} = [-270\ \ -30\ \ -20]^T$. The initial missile velocity $\boldsymbol{V}_{m0} = [1020\ 0\ 0]^T$ is defined in the missile reference frame. All units are expressed in the S.I. (metric) system. To emulate a guidance error in the previous phases of flight, the initial missile attitude was pointing directly at the initial target position. There is no initial missile angular velocity.

The initial target position $\boldsymbol{P}_{t0}$ in the inertial frame depends on the scenario. In the first scenario, the position is $\boldsymbol{P}_{t0} = [P_{t0x}\ \ 400\ \ -400]^T$ and the target approaches the missile head-on. In the second one, the position is $\boldsymbol{P}_{t0} = [P_{t0x}\ \ -800\ \ -400]^T$ and in a tail chase the target initially attempts to outrun the missile. In both, P_{t0x} can assume random values between 2000 and 4000 m, emulating the on-board radar detection range.

To evaluate miss distance, 100 realizations of each simulated scenario were run. Figures 7 and 8 present the miss distance compared with P_{t0x}. For scenario 1, the average miss distance is 3.2 m with standard deviation of 2.69 m and 98 % successful impact rate. For scenario 2, the average miss distance is 2.5 m with standard deviation of 2.68 m and 97 % impact rate. Successful impact rate considered an error of 10 m (estimated warhead lethal range).

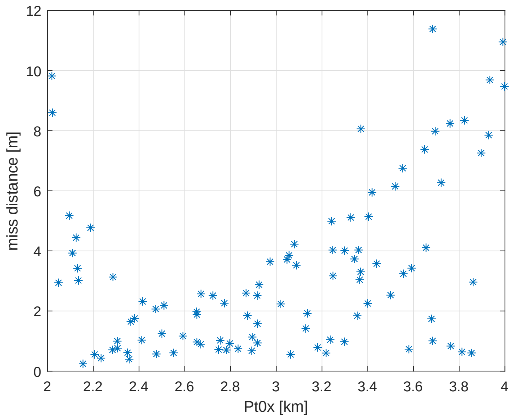

Figure 7. Results for scenario 1.

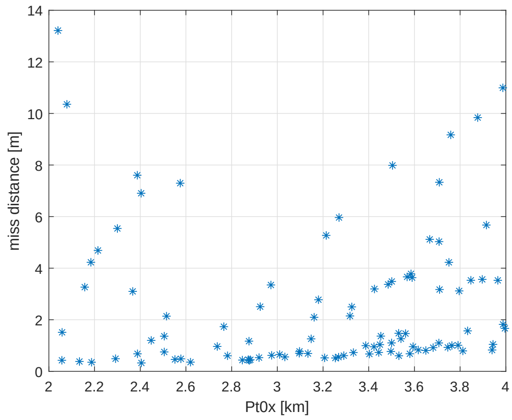

Figure 8. Results for scenario 2.

6. CONCLUSIONS

We propose a gain-scheduled, parameter-dependent autopilot based on four-block, loop-shaping H_∞ control with a LPV approach. The controller is dynamic and uses output feedback. For the loop-shaping synthesis, we propose weights with the same parameter dependence as the LPV plant model, describing them as polytopic system, in opposition to the classic non parameter-dependent weights. This allows shaping the LPV plant individually in the vertices as a natural extension of the usual loop-shaping for LPV systems. Tests were performed by the nonlinear simulation of a 6-degree-of-freedom surface-to-air missile. The average miss distance is less than 4 m for the simulated scenarios with a successful impact rate above 97% when a 10 m warhead lethality range and a 3-g maneuvering target are assumed.

7. REFERENCES

Apkarian, P. and Gahinet, P., 1995a. "A convex characterization of gain-scheduled H_∞ controllers". *IEEE Transactions on Automatic Control*, Vol. 40, No. 5, pp. 853–864.

Apkarian, P., Gahinet, P. and Becker, G., 1995b. "Self-scheduled H_∞ control of linear parameter-varying systems: a design example". *Automatica*, Vol. 31, No. 9, pp. 1251–1261.

Biannic, J.M. and Apkarian, P., 1999. "Missile autopilot design via a modified LPV synthesis technique". *Aerospace Science and Technology*, Vol. 3, No. 3, pp. 153–160.

Blake, W., 1998. *Missile Datcom: User's Manual-1997 FORTRAN 90 Revision*.

Evangelista, G.A., 2019. *Modelagem e Simulação de Mísseis Superfície-Ar*. Especialização, Instituto Tecnológico de Aeronáutica, São José dos Campos, SP.

Hiret, A., Duc, G. and Friang, J., 1999. "Self-scheduled H_∞ loop-shaping control of a missile". In *1999 European Control Conference (ECC)*. IEEE, pp. 1207–1212.

McFarlane, D. and Glover, K., 1990. "Robust controller design using normalized coprime factor plant description". In *Lecture notes in control and information Science*, Springer.

McFarlane, D. and Glover, K., 1992. "A loop-shaping design procedure using H_∞ synthesis". *IEEE transactions on automatic control*, Vol. 37, No. 6, pp. 759–769.

Natesan, K., Gu, D.W. and Postlethwaite, I., 2007. "Design of static H_∞ linear parameter varying controllers for unmanned aircraft". *Journal of guidance, control, and dynamics*, Vol. 30, No. 6, pp. 1822–1827.

Prempain, E., Postlethwaite, I. and Vorley, D., 2001. "A gain scheduled autopilot design for a bank-to-turn missile". In *2001 European Control Conference (ECC)*. IEEE, pp. 2052–2057.

Scherer, C., Gahinet, P. and Chilali, M., 1997. "Multiobjective output-feedback control via lmi optimization". *IEEE Transactions on automatic control*, Vol. 42, No. 7, pp. 896–911.

Shamma, J. and Athans, M., 1991. "Guaranteed properties of gain scheduled control for linear parameter-varying plants". *Automatica*, Vol. 27, No. 3, pp. 559–564.

Skogestad, S. and Postlethwaite, I., 2001. *Multivariable feedback control: analysis and design*, Vol. 2. Wiley New York.

Song, X., Song, J. and Ren, Z., 2013. "Robust LPV missile autopilot design with parameter dependent performance". In *2013 25th Chinese Control and Decision Conference (CCDC)*. IEEE, pp. 1998–2003.

Zhou, K., Doyle, J. and Glover, K., 1996. *Robust and optimal control*, Vol. 40. Prentice hall New Jersey.

8. RESPONSIBILITY NOTICE

The authors are solely responsible for the printed material included in this paper.